Chemical and Process Engineering 2012, 33 (1), 53-61
DOI: 10.2478/v10176-012-0005-2

EFFECTS OF STENT-GRAFT GEOMETRY AND BLOOD HEMATOCRIT ON HEMODYNAMIC IN ABDOMINAL AORTIC ANEURYSM

Andrzej Polańczyk[*1], Marek Podyma[1], Ludomir Stefańczyk[2], Ireneusz Zbiciński[1]

[1]Technical University of Lodz, Faculty of Process and Environmental Engineering, Department of Heat and Mass Transfer, ul. Wólczańska 213, 90-924 Łódź, Poland

[2]Medical University of Lodz, Department of Radiology and Diagnostic Imaging, ul. Kopcińskiego 22, 90-153 Łódź, Poland

CFD technique was used to determine the effect of a stent-graft spatial configuration and hematocrit value on blood flow hemodynamic and the risk of a stent-graft occlusion. Spatial configurations of an endovascular prosthesis placed in Abdominal Aortic Aneurysm (AAA) for numerical simulations were developed on the basis of AngioCT data for 10 patients. The results of calculations showed that narrows or angular bends in the prosthesis as well as increased hematocrit affects blood flow reducing velocity and WSS which might result in thrombus development.

Keywords: stent-graft, thrombosis, CFD, Abdominal Aortic Aneurysm, angular bend, narrowness

1. INTRODUCTION

The abdominal aortic aneurysm (AAA) is a potentially fatal condition of the abdominal aorta, which causes 1–2% of all male deaths over 65 years (Vliet and Boll, 1997). Moreover, AAA rupture leads to effusion of blood into abdominal cavity and may cause a sudden death (Aoki et al., 2009). Latest techniques of imaging e.g. ultrasonography, computer tomography or magnetic resonance enable a quick diagnosis of patients with AAA suspicion (Polanczyk et al., 2010). The treatment includes endovascular insertion of prosthesis whose role is to decrease stresses induced by blood flow on the impaired aorta's wall (Keyhani et al., 2009). Previously, Jung and Hassanein (2008), demonstrated in three-phase blood flow through a vessel that a higher blood leukocyte concentration correlates with a relatively low wall shear stress (WSS) near the stenosis having a high WSS which was in line with Liu et al. (2007) who noticed that for the arteries with stenosis the WSS at the inner wall peaks at the neck of the stenosis and reaches the minimum in the post-stenosis region, and then recovers gradually in the downstream until it levels off (Liu et al., 2007).

However, narrowness or angular bends in a stent-graft, especially in the iliac arteries, are common to occur. This may lead to blood flow disturbances and local hemodynamic changes. Therefore, in order to minimise post-operative complications after an endovascular prosthesis placement to AAA, constant modernisation and development of new solutions in the production of stent-grafts is observed (Owens, 2006). Hence computational analyses of this problem become helpful in minimising postoperative complications and computational fluid dynamic (CFD) is a useful tool to optimise the position of endovascular prosthesis and its proper spatial configuration (Berry et al., 2000).

*Corresponding author, e-mail: andrzej.polanczyk@gmail.com

2. SIMULATION RESULTS

2.1. Aim

The purpose of our work was to investigate the influence of geometry of a stent-graft in relation to blood hematocrit on plaque development.

2.2. Material and Methods

Computational Fluid Dynamic (CFD) is a widely used technique to simulate and analyse flow dynamic. From the wide range of CFD software available on the market we chose ANSYS FLUENT 12.1. In our study it was used to analyse the problem of blood coagulation in a stent-graft placed in the abdominal part of aorta. AngioCT data from 10 patients, at the age 50±10 years, and the 3DDoctor software were used to prepare a spatial configuration of an endovascular prosthesis placed in Abdominal Aortic Aneurysm. The results were analysed and the mean value from 10 cases was calculated. This enabled us to see the tendency of changes the in the analysed parameters. Calculations for one representative patient were selected and presented in Figures 2-7. This data showed general trends of changes in velocity, viscosity and wall shear stress in the whole analysed group. AngioCT data were provided by the Department of Cardiovascular Surgery Medical University of Lodz.

Gambit 2.2.30 software was used to elaborate geometry for blood flow calculation in analysed areas. The number of tetrahedral mesh elements for a particular endovascular prosthesis depended on the individual prosthesis geometry and changed from 400,000 to 500,000. ANSYS FLUENT 12.1 software was used to carry out CFD simulations. The walls of the analysed veins were treated as rigid surfaces. The investigated spatial configuration of the endovascular prosthesis had one inlet at the top and two outlets at the bottom (Fig.1). The boundary conditions were: for the inlet a velocity profile as a function of time and for outlet a pressure at the outlet. This provided us with a constant static pressure value on the outlet. Dimensions of the inlet and outlets for the presented case were: the characteristic inlet diameter of around 2 cm, the outlet diameters for the leg with narrowness of around 1.2 cm and for the leg without narrowness of 1.5 cm. The characteristic diameter of narrowness region was around 1.05 cm.

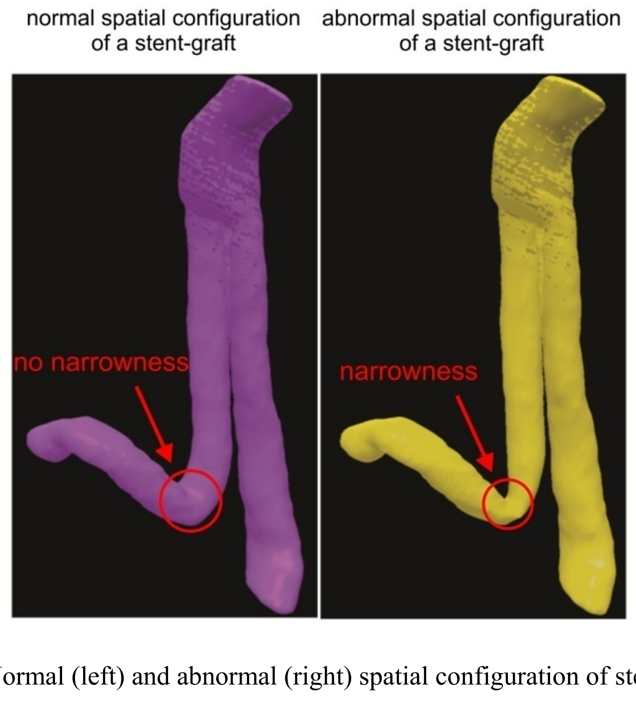

Fig. 1. Normal (left) and abnormal (right) spatial configuration of stent-graft

We focused on the influence of blood hemodynamics in places of narrows or angular bends in the endovascular prosthesis (Fig.1). During the calculation process the following numerical parameters were monitored: velocity, flow rate and viscosity distribution in the analysed domains and Wall Shear Stress (WSS) on the wall of the endovascular prosthesis.

We assumed pulsating character of blood flow as a boundary condition at the inlet of the analysed spatial configuration of the endovascular prosthesis. Pulsating character of blood flow was taken from Doppler procedure performed on a regular basis. The calculation time was equal to 1 second to ensure that it included one heart cycle. Moreover, we treated blood flow as laminar flow which was taken from Reynolds and Womerslay numbers available in the literature.

Mechanical properties of blood depended on red blood cells (RBCs) concentration in blood, which was described as a function of hematocrit (*Htc*) (Eq.1) (Polanczyk et al., 2010). *Htc* represents volumetric concentration of erythrocytes in a volume of whole human blood.

$$Htc = \frac{V_e}{V_b} \tag{1}$$

Htc is a parameter which has an influence on blood viscosity. An increase in *Htc* value results in an increase of blood viscosity and therefore, a decrease of blood velocity. This may result in an increased risk of blood coagulation. To monitor hemodynamic changes *Htc* values were changed at the range of 30% ÷ 60%. Following Hoskins et al. (2008) blood density was assumed as a constant value of 1040 kg/m3. Because of the high number of cells and the particulate nature of RBCs, whole blood exhibits non-Newtonian rheology and belongs to non-Newtonian liquids group diluted with an increased value of shear velocity, γ. Because of that Quemada's model was used to describe rheological properties of blood (Eq.2 and Eq.3) (Polanczyk et al., 2010).

$$\eta = \eta_p \left(1 - \frac{K \cdot Htc}{2}\right)^{-2} \tag{2}$$

$$K = \frac{k_0 + k_\infty \left(\frac{\gamma}{\gamma_c}\right)^{1/2}}{1 + \left(\frac{\gamma}{\gamma_c}\right)^{1/2}} \tag{3}$$

Parameters, k_0, k_∞ (Table 1), describing inner viscosity of erythrocytes, were chosen for neutral and infinity shear velocity respectively (Marcinkowska-Gapińska et al., 2007).

The moment of thrombus appearance was determined on the basis of critical shear stress below which viscosity was high enough to thrombus appearance. The γ_c parameter (Eq.3) is a critical value above which erythrocytes agglomeration process start. (Bębenek, 1999).

Table 1. Rheological parameters of blood for Quemada's model (Bębenek, 1999)

Htc	k_0	k_∞	γ_c
0.3	5.3	1.9	1.0
0.4	4.4	1.7	2.0
0.5	3.6	1.7	4.0
0.6	3.0	1.5	7.3
0.7	2.6	1.5	14.4
0.8	2.4	1.3	27.9

2.3. Results and discussion

Distribution of blood velocity, viscosity and wall shear stress during blood flow simulation through AAA with endovascular prosthesis inside was analysed and presented in Table 2.

Although our study showed that Reynolds values were within laminar flow, the values were different depending on the narrowness appearance. For a branch with narrowness it was around 70 and 150 for a branch without narrowness.

Table 2. Hematocrit influence on blood flow rate, viscosity and WSS in the areas with narrowness vs. without narrowness. Mean ±SD. % - percentage change in blood flow between branch with and without narrowness

Hematocrit *Htc* [-]	Change of flow rate [%]	Change of viscosity [%]	Change of WSS [%]
0.3	57 ± 11	5 ± 7	37 ± 10
0.4	59 ± 9	7 ± 6	40 ± 8
0.5	61 ± 9.5	10 ± 7	43 ± 7.5
0.6	63 ± 8	12 ± 6	45 ± 7

2.4. Flow rate

Velocity distribution enables to predict blood stagnation areas in the investigated abdominal part of aorta (Fig.2).

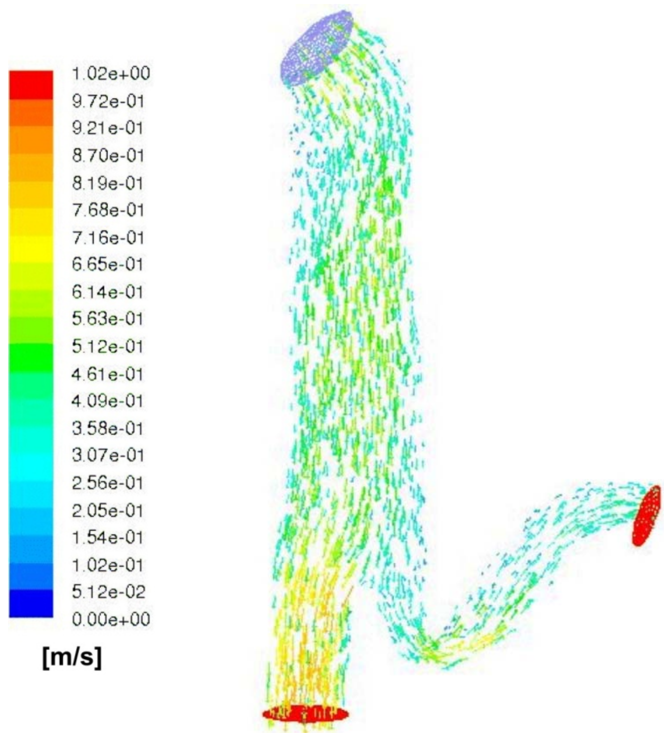

Fig. 2. Blood velocity vectors for 0.10 s period of time for *Htc* = 50%. Data for one representative patient

An increased value of *Htc* was connected with a higher value of viscosity that involved higher drag forces. In our study the flow rate distribution was different in a vessel with or without narrowness.

It was observed that with an increasing value of *Htc*, the flow rate in a branch with narrowness was decreasing. This supports the fact that a branch without narrowness becomes a main duct responsible for directing blood to the lower part of human body.

Therefore, a lower value of the blood flow rate in a function of higher *Htc* was observed in narrowness. Moreover, it was noticed that the branch without narrowing had much higher values of the flow rate compared with the branch with a narrow place (Fig. 3a, b).

a)

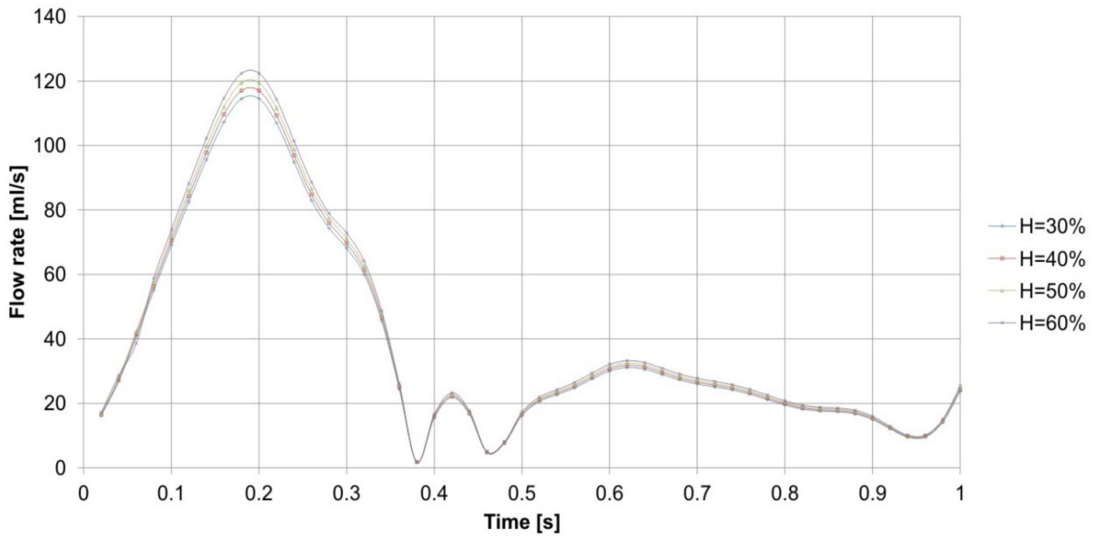

b)

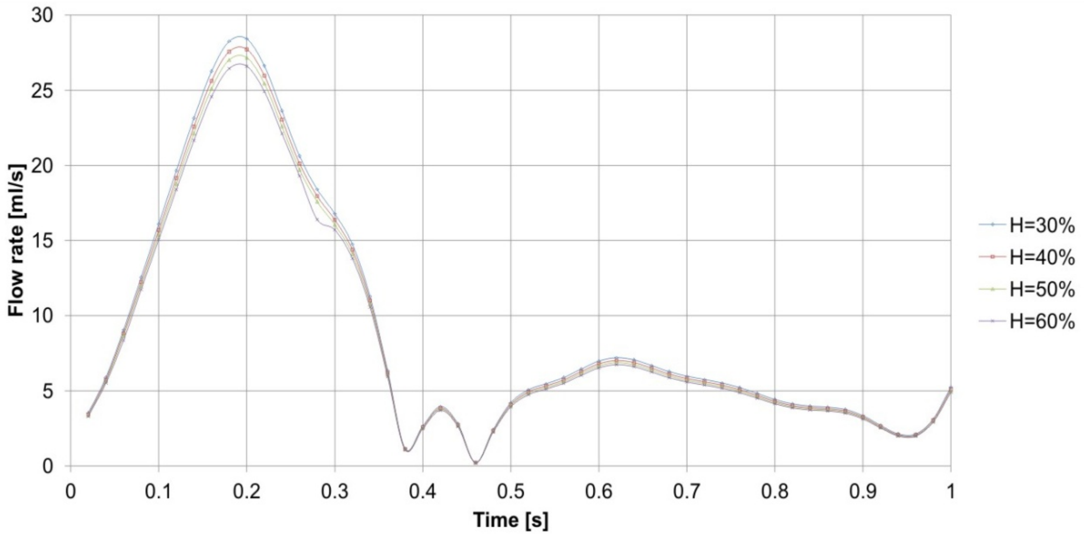

Fig. 3. Blood flow distribution in: a) branch without, b) with narrowness. Data for one representative patient

The highest value of the flow rate for all the analysed cases was observed at 0.18 second of blood flow. We assume that this phenomena correlate with the heart cycle as near to this time period heart contrition appears. For *Htc* = 30% average value of the blood flow rate observed for a branch with narrowness was 57% higher compared with a branch without narrowness. Moreover, with an increasing value of *Htc* differences in the blood flow rate also increased. For *Htc* = 60% the average value of differences increased up to 63%.

2.5. Blood viscosity

Blood viscosity distribution enables to predict places with a high risk of thrombus appearance. In our study an increasing value of *Htc* (from 30% to 60%) corresponded to increased viscosity in a branch with narrowness (Fig.4) and is correlated with a lower value of the blood flow rate followed by increased drag forces.

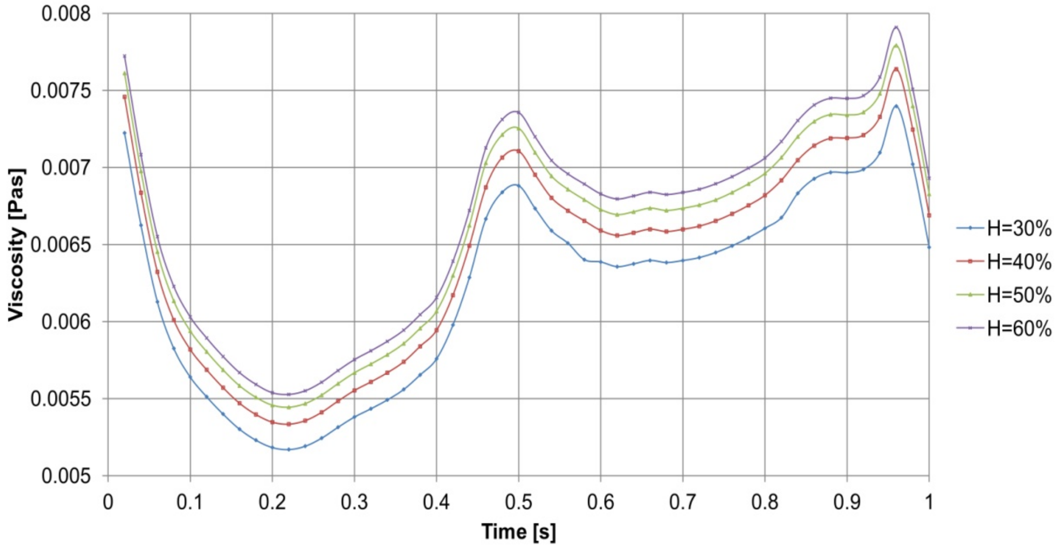

Fig. 4. Viscosity distribution in branch with narrowness. Data for one representative patient

Moreover, in our work in the area without narrowness blood viscosity decreased and simultaneously *Htc* value increased which was correlated with the blood flow. A higher flow rate that reduced blood viscosity appeared in the branch without narrowness (Fig.5).

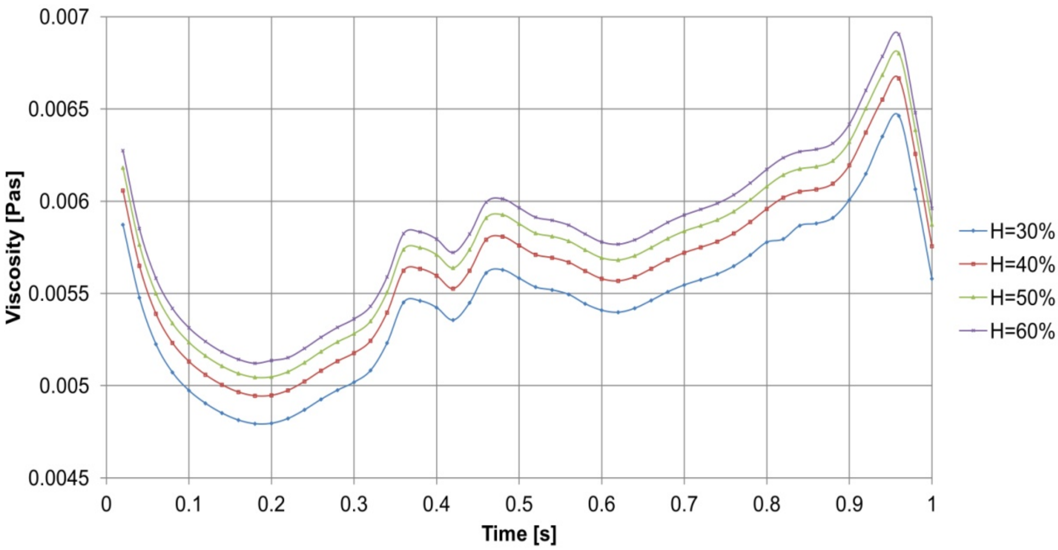

Fig. 5. Viscosity distribution in branch without narrowness. Data for one representative patient

Therefore, in narrowness an increasing value of blood viscosity in a function of higher *Htc* was observed. It was noticed that differences in blood viscosity for both branches with and without narrowness increased simultaneously with an increasing value of *Htc*. For *Htc* = 30% the average value of blood viscosity observed for the branch with narrowness was 5% higher compared with the branch without narrowness.

Our research also showed that increased *Htc* values were accompanied by increased viscosity values in a narrowed vessel. Recent studies report that regions of flow recirculation formed near the wall due to rapid changes in the flow rate, low fluid viscosity, and the curvature of the sinus. Moreover, within such recirculation regions, blood moves in the direction opposite to the mean flow increasing the probability of plaque deposition (Nguyen et al., 2008).

2.6. Wall Shear Stress

We observed that with an increasing value of *Htc* the average value of WSS for the branch with narrowness decreased. On the contrary in the branch without narrowness higher values of WSS were accompanied by higher values of the blood flow rate (Fig.6).

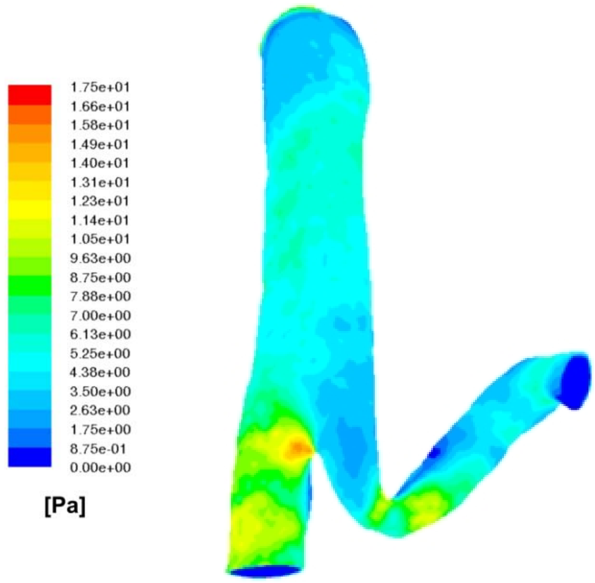

Fig. 6. Wall shear stress (WSS) contours for 0.10s period of time for *Htc* = 50%. Data for one representative patient

Additionally higher values of WSS were observed for areas with lower viscosity, and similarly, higher flow rate. Moreover, higher values of *Htc* in the branch with narrowing showed much lower values of WSS which correlated with a decreased blood flow and increased viscosity distribution (Fig.7). Therefore, in areas of low shear velocity low WSS values were observed.

Our stimulations also showed that for the branch without narrowness a higher value of WSS correlated with the blood flow rate and viscosity distribution. For the branch without narrowness (Fig.7) blood flow rate was higher and viscosity had lower values compared to the branch with narrowness. Therefore, in narrowness a decreasing value of WSS is a function of higher *Htc* was observed. Generally higher WSS characterised areas where the probability of blood coagulation was higher.

Our results indicated that an increasing value of *Htc* involved higher differences of WSS between the branches with and without narrowness. The average value of WSS observed for *Htc* = 30% for the branch without narrowness was 37% higher than in the branch with narrowness. Moreover, with an increased value of *Htc* WSS differences also increased. For *Htc* = 60% the average value of differences increased up to 45%.

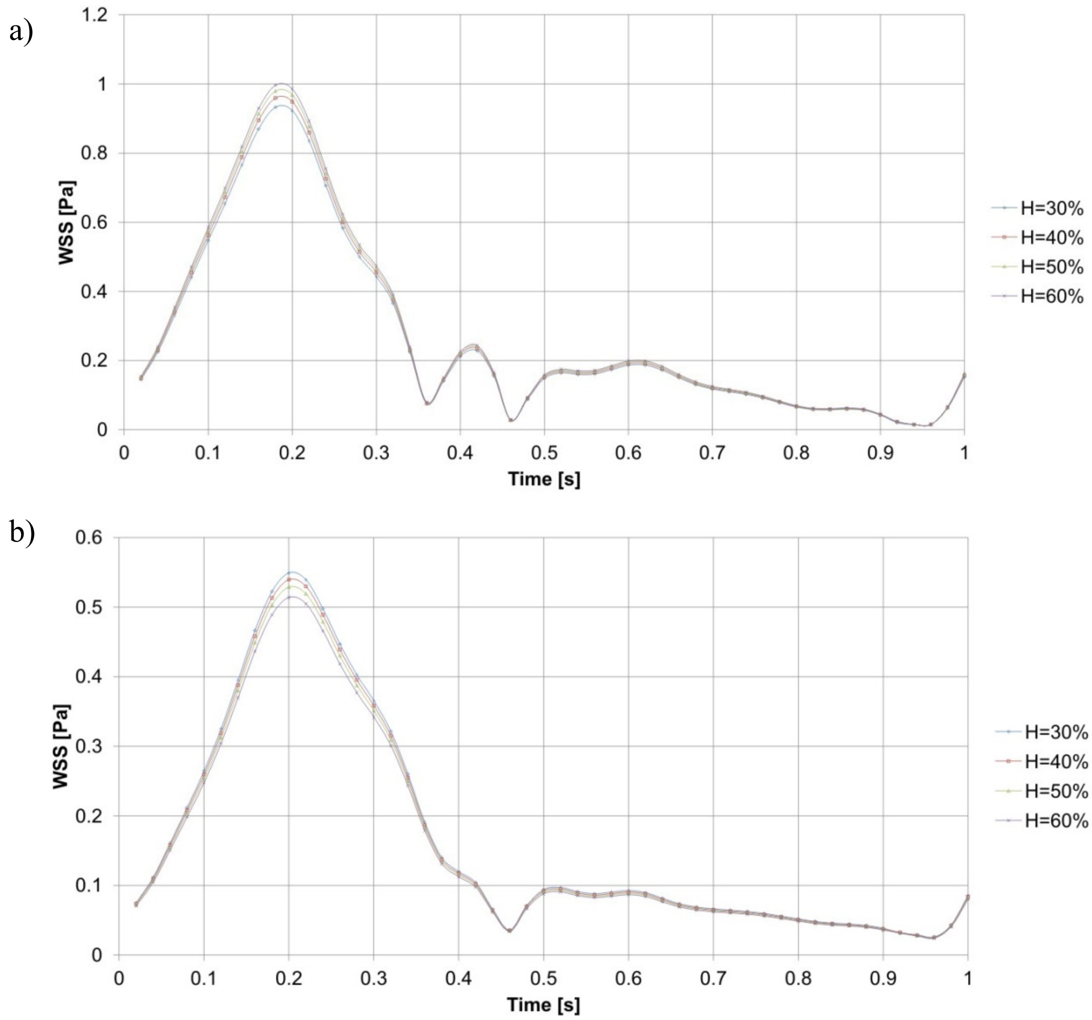

Fig. 7. WSS distribution in: a) branch without b) with narrowness. Data for one representative patient

3. CONCLUSIONS

CFD simulation proved an effect of spatial configuration of a stent-graft installed in AAA on blood hemodynamics. The results indicated that narrows and angular bends of the endovascular prosthesis influence hemodynamics reducing blood velocity in vessels. An increase in hematocrit in the area of narrows and angular bends in the iliac part of the endovascular prosthesis leads to a reduction in the blood flow rate and WSS which induce an increase of viscosity and the risk of plaque formation and occlusion.

The study was supported by Grant No. 2011/35 from the Technical University of Lodz.

SYMBOLS

Htc	hematocrit, parameter of erythrocytes content in blood, -
K	inner viscosity of erythrocytes, -
k_0	parameters describing blood behaviour, -
k_∞	parameters describing blood behaviour, -

Greek symbols

γ	shear rate, 1/s
γ_c	boundary shear rate, 1/s
η	blood viscosity, Pa·s
η_p	plasma viscosity, Pa·s
τ	shear stress, Pa

REFERENCES

Aoki Y., Takamiya M., Niitsu H., Fujita S., Saigusa K., 2009. An autopsy case of aortitis resulting in sudden death due to a rupture of aneurysm of the aortic sinus. *Leg. Med. (Tokyo)*, 11, 33-36. DOI: 10.1016/j.legalmed.2008.07.002.

Bębenek B., 1999. *Flows in a circulatory system*. Wydawnictwo Politechniki Krakowskiej, Cracow, 350 (in Polish).

Berry J., Santamarina A., Routh W., 2000. Experimental and computational flow evaluation of coronary stents. *Ann. Biomed. Eng.*, 28, 386-398. DOI 10.1114/1.276.

Hoskins P. R., 2008. Simulation and validation of arterial ultrasound imaging and blood flow. *Ultrasound. Med. Biol.*, 34, 693-717. DOI: 10.1016/j.ultrasmedbio.2007.10.017.

Jung J., Hassanein A., 2008. Three-phase CFD analytical modeling of blood flow. *Med. Eng. Phys.*, 30, 91–103. DOI: 10.1016/j.medengphy.2006.12.004.

Keyhani K., Estrera A. L., Safi H. J., 2009. Azizzadeh A., Endovascular repair of traumatic aortic injury in a pediatric patient. *J. Vasc. Surg.*, 50, 652-654. DOI: 10.1016/j.j.vs.2009.04.040.

Liu B., 2007. The influences of stenosis on the downstream flow pattern in curved arteries, *Med. Eng. Phys.*, 29, 868-876. DOI: 10.1016/j.medengphy.2006.09.009.

Owens R. G., 2006. A new microstructure-based constitutive model for human blood. *J. Non-Newtonian Fluid Mech.*, 140, 57-70. DOI: 10.1016/j.jnnfm.2006.D1.015.

Marcinkowska-Gapińska A., Gapiński J., Elikowski W., Jaroszyk F., Kubisz L., 2007. Comparison of three rheological models of shear flow behavior studied on blood samples from post-infarction patients. *Med. Biol. Eng. Comput.*, 45, 837-844. DOI: 10.1007/s11517-007-0236-4.

Nguyen K. T., Clark C. D., Chancellor T. J., Papavassiliou D. V., 2008. Carotid geometry effects on blood flow and on risk for vascular disease, *J. Biomech.,* 41, 11-19. DOI: 10.1016/j.jbiomech. 2007.08.D12.

Polańczyk A., Piechota A., 2010. CFD simulations of blood flow through abdominal part of aorta. *Chall. Modern Technol.*, 1, 34-39.

Polańczyk A., Zbiciński I., 2010. Blood flow simulation through endovascular prosthesis to patients with Abdominal Aortic Aneurysm, *Procesnie Technika*, 1, 105-115.

Vliet J.A., Boll A.P., 1997. Abdominal aortic aneurysm. *Lancet,* 349, 863-6. DOI: 10.1016/S0140-6736(96)07282-D.

Received 30 September 2011
Received in revised form 30 December 2011
Accepted 30 December 2011